

Tunable Diode Laser Study of the Reaction $\text{OH} + \text{ClO} \rightarrow \text{HCl} + \text{O}_2$

G. S. Tyndall,* C. S. Kegley-Owen,† J. J. Orlando, and A. Fried

Atmospheric Chemistry Division, National Center for Atmospheric Research, P.O. Box 3000, Boulder, Colorado 80307

Received: September 5, 2001; In Final Form: December 6, 2001

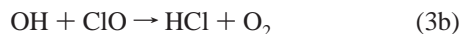
Time-resolved tunable diode laser spectroscopy has been used to measure the production of HCl in the reaction of OH and ClO radicals. The OH and ClO radicals were formed from the 308 nm laser photolysis of mixtures containing O_3 , Cl_2 , and H_2O . Computer simulations of the chemistry were used to derive a rate coefficient of $(1.25 \pm 0.45) \times 10^{-12} \text{ cm}^3 \text{ molecule}^{-1} \text{ s}^{-1}$ for the title reaction at 298 K. This reaction rate, which corresponds to a branching fraction of $(6.5 \pm 3.0)\%$ relative to the currently recommended rate coefficient for the overall reaction, confirms that the reaction will have a substantial impact on the partitioning of chlorine compounds in the stratosphere.

Introduction

The concentration of ozone in the stratosphere is governed by a delicate balance between its production through oxygen photolysis and its loss via catalytic free radical cycles. The major cycles involve nitrogen oxides (NO and NO_2), odd hydrogen radicals (OH and HO_2), and halogen-containing radicals (Cl, ClO, Br, and BrO). The halogen species in the stratosphere are predominantly man-made and consequently have been changing on a much faster time scale than the other species. In the mid-stratosphere, the major loss of ozone is currently due to chlorine atom chemistry.^{1–3} Loss of ozone is tempered by the formation of reservoir species which temporarily convert the active species into an inactive form. In the case of chlorine, the reservoirs are (in order of decreasing lifetime) HCl, ClONO₂ and HOCl. The first of these, HCl, does not undergo photolysis to any extent in the lower- to mid-stratosphere and reacts only slowly with OH, and so is a particularly effective sink. The main pathways for formation of HCl in the stratosphere are through reaction of chlorine atoms with methane and formaldehyde:



Any reaction which converts active chlorine species to HCl will thus be of potential importance in the mid-stratosphere. The reaction of OH with ClO (3) offers a possible mechanism for this to occur. The major reaction pathway forms $\text{HO}_2 + \text{Cl}$, but it is also thermodynamically possible to form $\text{HCl} + \text{O}_2$ in reaction 3b, which is exothermic by 56 kcal mol⁻¹ to produce $\text{O}_2(^3\Sigma)$, or by 33 kcal mol⁻¹ to produce $\text{O}_2(^1\Delta)$:



The latter pathway removes members of both the odd hydrogen and active chlorine families. Brasseur and co-workers⁴ were among the first to suggest in the mid-1980s that if channel 3b

occurs with a yield of only a few percent, it is capable of exerting an influence on the ozone levels. Inclusion of the reaction in atmospheric models was found to partially account for the underprediction of ozone at 40 km altitude and also to improve model estimates of the magnitude of the observed decadal ozone trends.^{5–8}

Stronger evidence for the occurrence of channel 3b came in the way of satellite measurements of the partitioning between members of the chlorine family, ClO, ClONO₂ and HCl. Such measurements indicated a substantially improved fit for models if reaction 3b was included with a branching ratio of ~7%.^{8–11} It has also been pointed out that reaction 3b can play a role in the rate of recovery of the ozone hole by accelerating the conversion of active chlorine to HCl under denitrified conditions, when chlorine nitrate concentrations are low and ClO high.¹²

Laboratory measurements of the rate coefficient of reaction 3 have been available since the late 1970s.^{13–21} The most recent determinations^{19–21} seem to indicate a higher rate coefficient than thought previously. A number of the early studies^{13,15,16} quantified k_{3a} via HO_2 production, inferring branching fractions k_{3b}/k_3 that were less than 0.15. The exception was the study of Poulet et al.,¹⁷ in which HCl yields of <2% were reported. However, large corrections had to be made for secondary production of HCl by the reaction $\text{Cl} + \text{HO}_2$.

More recently, three groups have reported direct studies of reaction 3b. Lipson et al.^{18,22} used a high-pressure flow tube with chemical ionization mass spectrometry and found yields of 7% relative to their measurement of k_3 . Wang and Keyser²³ used a low-pressure discharge-flow system with tunable diode laser detection and reported an absolute HCl yield (independent of k_3) of 9%. Most recently, Bedjanian et al.²⁰ reported a yield of 3.5% at room temperature. All these studies used flow tubes, which can be subject to loss or production of “sticky” compounds such as HCl. The present study uses a different approach, by producing HCl in a flash system and observing its formation on a time scale faster than diffusion to or from the walls of the vessel. In this sense, it can be considered a “wall-less” reactor. Both OH and ClO radicals were produced by the same excimer laser pulse, and HCl was detected by time-resolved tunable diode laser spectroscopy in direct absorption. Diode laser absorption is a sensitive and specific technique that can be used in time-resolved mode for either free radicals or

* Corresponding author. Tel: 303-497-1472. Fax: 303-497-1411. E-mail: tyndall@acd.ucar.edu.

† Present address: Department of Chemistry, University of Nebraska, Kearney, NE 68849.

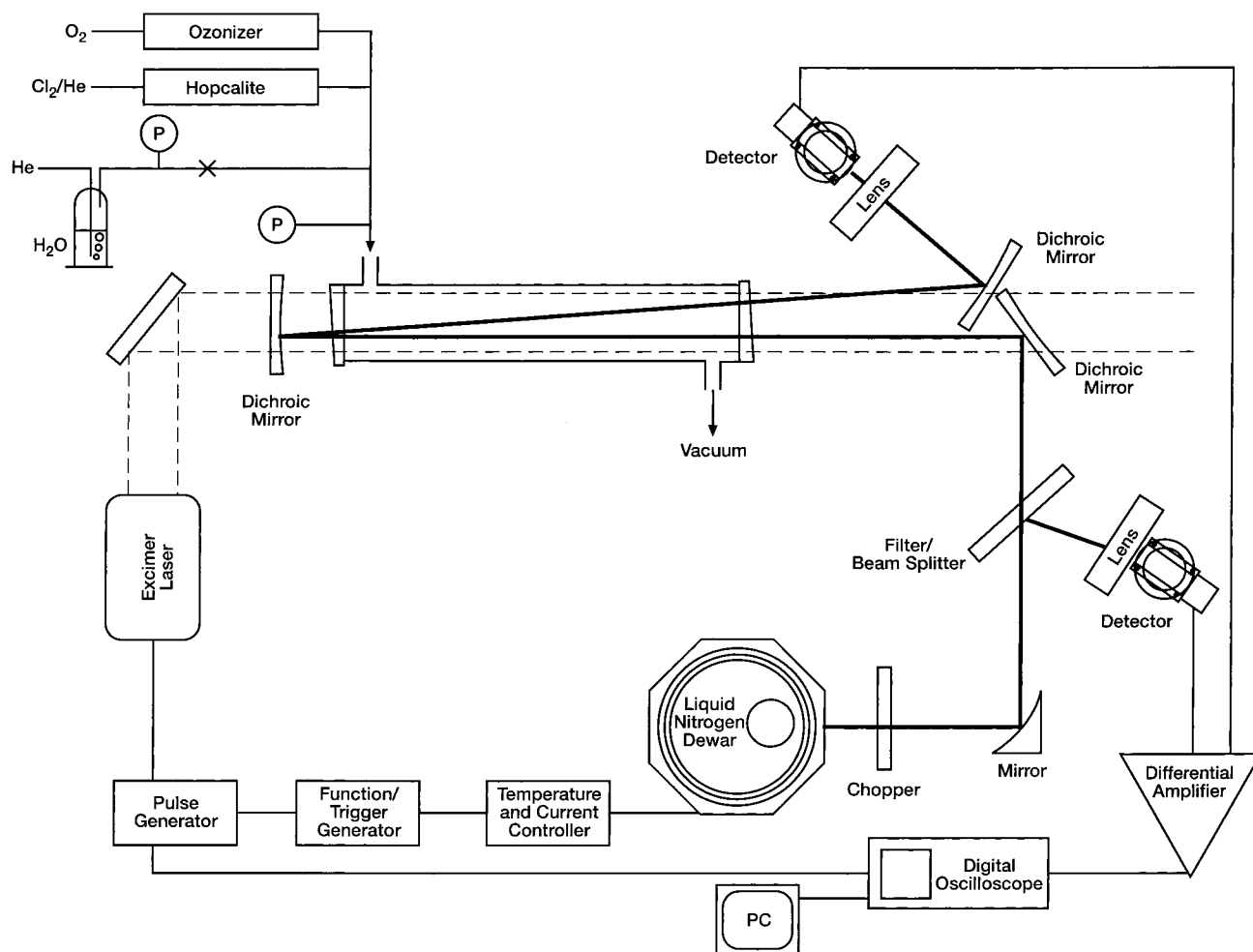


Figure 1. Schematic of experimental setup. The laser diode is housed in the liquid nitrogen dewar pointing downward. A gold-coated off-axis ellipsoidal mirror located under the dewar collects and focuses the beam, and the second one (shown) collimates it through the cell.

stable products.^{24–26} The final value for the rate coefficient of reaction 3b was obtained by computer modeling of the total amount of HCl produced, taking into account primary and secondary HCl sources.

Experimental Section

The experiments involved using tunable diode laser (TDL) spectroscopy to measure the HCl produced by pulsed excimer laser photolysis.²⁴ The experiments were carried out in a 47.7 cm jacketed cell, 5 cm in internal diameter, fitted with wedged BaF₂ windows (Figure 1). External dielectric-coated mirrors (Creative Optics, Texas) reflected the TDL beam twice through the cell to give an optical path length of 95.4 cm. The dielectric mirrors transmitted UV radiation, allowing photolysis of the gas mixture down the length of the cell. After passing through the cell, the TDL beam was detected on a liquid nitrogen cooled InSb detector/preamplifier (Cincinnati Electronics SDD-7854). A band-pass filter positioned after the TDL focusing optics protected the diode from scattered UV light. The filter, set at 45° to the path of the laser beam, also served to reflect a small fraction of the beam onto a second InSb detector which was used to remove baseline fluctuations. Both detectors were fitted with long-pass filters to remove scattered excimer light. Transient signals from the detectors were averaged in a LeCroy 9450 digital oscilloscope and sent to a PC for analysis.

The radiation used to detect the reaction product HCl was generated using a quaternary lead-salt diode laser, cooled by

liquid nitrogen. The exact temperature and current of the diode (typically 81 K and 0.35 A) were adjusted externally to control the output wavelength of the laser, which was swept by applying a sawtooth ramp to the current at a frequency of 1 kHz. The ramp provided both the spectroscopic frequency axis within a given sweep, and the kinetic time base for the experiments via the generation of consecutive sweeps through the HCl line 1 ms apart. The total DC laser power reaching the detector was measured several times a day by inserting a mechanical chopper at the primary focus of the beam (see Figure 1). The mode purity (which was ~96%) was checked from time to time by flowing HCl through the photolysis cell at a high enough concentration (>10¹⁴ molecule cm⁻³) to absorb >98% of the laser light. Secondary checks of mode purity were made at the start and finish of each day using a sealed cell containing a known amount of OCS.

The output of the laser was swept through the R(1) absorption line of HCl, allowing a differential (peak to baseline) signal to be measured in direct absorption. Sweeping the diode output reduced uncertainties potentially caused by transient (<2 ms) fluctuations in diode laser wavelength caused by electrical pick-up from the excimer laser pulse, or offset on the detector due to scattered excimer radiation. The sweep of the diode laser was synchronized to the excimer laser trigger so that the absorption was always measured at the same delay times relative to the excimer laser. Hence, the signal could be averaged over consecutive excimer laser flashes, and by averaging 50 traces,

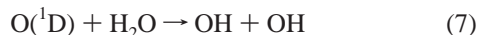
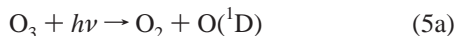
peak-to-peak noise levels of 1×10^{-5} absorbance units could be obtained, corresponding to about 3×10^9 HCl molecule cm^{-3} . The ultimate detection limit was governed by drifts in the laser output frequency, which caused the noncancellation of interference fringes.

The sweep current imposed on the diode corresponded to an amplitude of $\sim 0.11 \text{ cm}^{-1}$. The change in laser power associated with the sweep resulted in a sloping background which was often larger than the HCl absorption feature, limiting the number of bits available for recording the absorption. Two approaches were used to remove this background modulation. For HCl calibration experiments involving the photolysis of $\text{Cl}_2\text{-C}_2\text{H}_6\text{-O}_2$, concentrations of HCl in excess of 10^{12} molecule cm^{-3} were produced, and a single detector was used. Averages were alternately taken with Cl_2 present (signal) and without Cl_2 (background), and the background trace was digitally subtracted from the signal trace to remove the slope. For the measurement of the very small amounts of HCl in the OH + ClO experiments, two detectors were used. Part of the beam was picked off before entering the cell and sent to the reference detector. The output from both detectors was fed to a differential amplifier which subtracted the signals to remove the slope in real time. The resultant differential signal was amplified by a factor of 67, and the amplified signal was fed to the digital oscilloscope for averaging. Again, averages with and without Cl_2 present were subtracted digitally. Extensive tests showed that the amount of HCl measured in both direct and differentially amplified modes agreed in both peak height and integrated area and that the amplifier did not cause any clipping of the signal.

Even after averaging and digital subtraction, small fluctuations remained in the baseline associated with residual 120 Hz vibrations. These oscillations could be removed by co-adding the individual sweeps to provide one pre-photolysis and one post-photolysis measurement of HCl. Thus, the primary measured quantity was the change in HCl produced by a given [OH] and [ClO].

The reaction was initiated by a pulse from an excimer laser (Questek model 2440) operating at the 308 nm XeCl line. The excimer laser was positioned several meters from the reaction cell, so the UV beam was wide and filled the cell fairly uniformly. The laser power was measured using a pyroelectric power meter that was cross-calibrated against two meters of the disk-calorimeter type used by the NOAA Aeronomy lab (R. Talukdar, Pers. comm.). A 4- cm^2 square mask was used to map out and measure the fluence directly. Fluctuations over the beam profile were less than 5%. Excimer laser powers of 100–140 mJ/pulse were used, which resulted in fluences of 1.0–1.5 mJ cm^{-2} measured behind the cell.

The reactants ClO and OH radicals were produced concurrently by the flash photolysis of mixtures containing Cl_2 , O_3 , and H_2O



The main carrier gas was a flow of helium (250–400 sccm), which was passed through an aspirator near room temperature to saturate it with water. The aspirator stood in a water bath,

the temperature of which was constantly monitored. At such flow rates, it can safely be assumed that the helium was fully saturated with H_2O vapor.²⁷ The flow of water vapor was calculated using tabulated vapor pressures²⁸ and the measured total pressure in the aspirator. The water vapor concentration was also measured in the reaction cell using absorption of the mercury emission line at 184.9 nm as described previously;²⁷ the measured water vapor agreed with that calculated from its vapor pressure to within 2%. Chlorine from a lecture bottle was made into a 10% mix in helium; the mole fraction of Cl_2 was occasionally checked off-line using a UV–visible diode array spectrometer. A flow of 40–80 sccm ultrahigh purity O_2 was passed through a dry ice trap and then through an ozonizer which was known to produce 3.8% O_3 . The ozone mixing ratio in the absorption cell was also checked daily using absorption of a 254-nm Penray Hg lamp. UV absorption cross sections and quantum yields for Cl_2 and O_3 were taken from the NASA JPL compilation.²⁹ Pressures in the reaction cell and the water bubbler were measured using capacitance manometers. Calculated residence times in the cell were 3–5 s. Flows were maintained using mass flow controllers that had been calibrated using a commercial bubble meter for the exact gases and range of flow rates used. Gases used, with purities were: Cl_2 (UHP 99.5%, Matheson), He (UHP, US Welding), O_2 (UHP, US Welding), and H_2O (deionized in house, 18 Mohm).

Since the branching ratio to produce HCl was expected to be small, the utmost care had to be taken to minimize background HCl in the gas flow and also any HCl produced by secondary reactions. The Cl_2 was found to contain about 100 ppm HCl, which resulted in background levels roughly 10 times higher than the amount produced from the reaction. Initial attempts to purify the Cl_2 by distillation were not very successful. A better solution was found to be the inclusion in the flow path of a short glass trap containing a small amount (about 100 mg) of Hopcalite catalyst (Cu-Mn-O) held between glass wool plugs. By trial and error, it was found that an appropriate amount could be used that removed essentially 100% of the HCl while still passing the Cl_2 (as verified by UV spectroscopy). Since Hopcalite is used in atmospheric chemistry field experiments as an ozone “killer”, it was obviously necessary to avoid passing the ozonized O_2 through the trap (see Figure 1).

HCl was detected using the R(1) line of the fundamental stretching mode of H^{35}Cl at 2925.897 cm^{-1} . The integrated line strength S_j was taken from the HITRAN listing,³⁰ which is in turn based on the work of Pine et al.³¹ For the R(1) line of the HCl fundamental, S_j is $4.19 \times 10^{-19} \text{ cm molecule}^{-1}$, with an uncertainty of 2–3%. The HCl was quantified using both integrated line strength and peak-to-baseline cross sections (see next section). The absolute HCl could be compared to the amount of HCl produced in situ by the reaction of Cl atoms with C_2H_6 . The frequency of the diode laser output was calibrated relative to well-characterized OCS absorption lines.

For the majority of the experiments, a time base of 20 ms was used with a 1 kHz sweep rate of the diode laser, and 800 digitized pixels were recorded (25 μs per pixel). Six diode laser sweeps were acquired prior to the excimer pulse and 12 after. Due to the rapidity of the chemistry, this only allowed the net change of HCl to be measured. For some experiments, however, the sweep rate was increased to 4 kHz to allow time-resolved HCl profiles to be acquired. The repetition rate of the excimer laser was 0.2 Hz, allowing the contents of the cell to be swept out between pulses. This was necessary to avoid the build-up of both HCl and ClO (which reacts only slowly with itself).

The Cl₂–C₂H₆ experiments could be used to show that HCl from the previous pulse had been removed before data acquisition began and that any residual HCl observed was residual in the Cl₂ flow breaking through the Hopcalite filter.

Results

Calibration of HCl. The most critical parameters in the determination of k_{3b} are the quantification of HCl and the measurement of the excimer laser fluence (i.e., the determination of OH and ClO). Particular care was taken to characterize the cross section of HCl under the conditions used, and to relate the excimer laser fluence to the amount of HCl produced in a known reaction. In this way, the system was internally calibrated, and systematic errors were reduced. The HCl concentration was determined using either peak cross section or integrated line strengths.

Measurement of HCl Using Integrated Line Strengths. The concentration of HCl was most readily derived experimentally from the integrated area under the resolved rotational line used. Raw voltages were converted to absorbance, A , using the chopped single-mode laser power and the Beer–Lambert law. The tuning rate of the diode laser with current was measured using a germanium etalon with a free spectral range of 0.015 98 cm⁻¹, calculated from the refractive index at the exact frequency and laboratory temperature used. The HCl R(1) line was recorded using an expanded oscilloscope time base with 400 pixels per sweep, enabling the peak to be fully resolved. The absorbance was integrated over a defined number of pixels, dp , and converted to concentration using equation A

$$[\text{HCl}] = \frac{1}{S_j l} \frac{\partial \omega}{\partial p} \int A dp = \frac{A_0}{\sigma_0 l} \quad (\text{A})$$

where S_j is the integrated line strength, l is the path length, $\partial \omega / \partial p$ is the diode tuning rate per pixel, A_0 is the absorbance at line center, and σ_0 the peak absorption cross section.

For the kinetics measurements, a time base of 20 ms per trace was used, so multiple sweeps through the HCl line were recorded, separated by 1 ms. Using this slower time base, about 15 pixels were recorded across the HCl absorption line. The area under the absorption feature was integrated using the central 11 pixels, defining a baseline starting 7 pixels on either side of the peak. By comparing traces recorded under the same conditions but with slow and fast time bases, it was shown that the area defined in the kinetics scans captured >95% of the true area for all except the experiments at 40 Torr with added H₂O, where the line width is largest. For such cases a correction was made for the “missing” area. The sweep routine was also tested using known flows of CH₄, which is not lost in flow controllers. The CH₄ concentrations derived using the HITRAN line strengths (four lines near 2926.8 cm⁻¹) agreed with those from flows to within a few percent. The measured areas were also found to be independent of whether the differential amplifier was used or not.

Calculation of HCl Cross Sections. The concentration of HCl was also derived using peak absorption at line center. First, the peak HCl absorption cross section was calculated at 10 different pressures of N₂ between 0 and 40 Torr using a Voigt profile and the broadening coefficients given by Pine and Looney.³² The variation of this cross section with pressure was then fitted with a second-order polynomial to allow the cross section to be interpolated at an arbitrary pressure. Then, using known or measured broadening parameters γ (as described below) for He, O₂, and H₂O, an equivalent pressure of N₂, P_{equ} ,

could be calculated for any given reaction mixture, and the corresponding cross section obtained:

$$P_{\text{equ}} = \frac{\gamma_{\text{He}} P_{\text{He}}}{\gamma_{\text{N}_2}} + \frac{\gamma_{\text{O}_2} P_{\text{O}_2}}{\gamma_{\text{N}_2}} + \frac{\gamma_{\text{H}_2\text{O}} P_{\text{H}_2\text{O}}}{\gamma_{\text{N}_2}} \quad (\text{B})$$

Broadening coefficients γ (half-width at half-maximum in cm⁻¹ atm⁻¹) for nitrogen and air are known with high accuracy as a function of rotational quantum number, J , from the work of Pine and Looney,³² from which a half-width for oxygen can be obtained. However, since most of the broadening in air is due to N₂, values of γ_{O_2} obtained in this manner may not be very accurate. Babrov et al.³³ measured broadening half-widths for pure O₂ and N₂, as a function of J at low resolution, and found a smooth trend of γ with rotational quantum number. Hence, the values for O₂ deduced from Pine and Looney were smoothed according to the trend given by the Babrov data. Broadening coefficients for HCl lines by helium, γ_{He} , have been measured by Rank et al.³⁴ and Babrov et al.³³ These values were used as the initial guesses for this work but optimized as described below.

Concentrations of HCl in different gas mixtures were derived from the integrated absorbance, as described in the previous section, and a peak absorption cross section was derived. A cross section was then calculated from the nonlinear fit of cross section versus N₂ pressure using an equivalent N₂ pressure as defined in eq B. The broadening coefficients were then varied to simultaneously minimize the differences between all the measured and calculated cross sections. Such line width measurements were made using both flowing mixtures of authentic HCl and HCl produced in situ from the photolysis of Cl₂–C₂H₆–O₂–He mixtures. In this way, broadening coefficients for H₂O could be determined and those for He and O₂ refined. The half-widths for broadening by He, O₂ and H₂O were found to be 0.026, 0.052, and 0.22 cm⁻¹ atm⁻¹, respectively, which can be compared to the literature values for He of 0.022³⁴ and 0.020³³ and for O₂ of 0.041³² and 0.051.³³ The coefficient $\gamma_{\text{H}_2\text{O}}$ is similar in magnitude to that for self-broadening of HCl, 0.24 cm⁻¹ atm⁻¹.³⁰ The broadening coefficients are expected to be accurate to about 20%. It should be noted, though, that values for γ were only determined under conditions closely resembling those where experiments were conducted and that they were only used to interpolate measured cross sections by a few percent to match experimental conditions. Hence, the results are not sensitive to the exact values of the broadening coefficients. The calculated Doppler-limited peak cross section of HCl R(1) at 296 K is 6.51 × 10⁻¹⁷ cm² molecule⁻¹. The measured HCl cross sections under the experimental conditions ranged from 4.85 to 3.55 × 10⁻¹⁷ cm² molecule⁻¹, depending on the total pressure and the amount of water vapor present.

In Situ Calibration of HCl. The reaction of Cl atoms with C₂H₆ was used to measure the amount of HCl produced by a given concentration of Cl₂ and excimer power. This reaction is known to be rapid and provided quantitative conversion of Cl atoms to HCl under the exact conditions of the OH + ClO experiment



The HCl concentration derived from the TDL absorption measurement was corrected for a small amount of regeneration

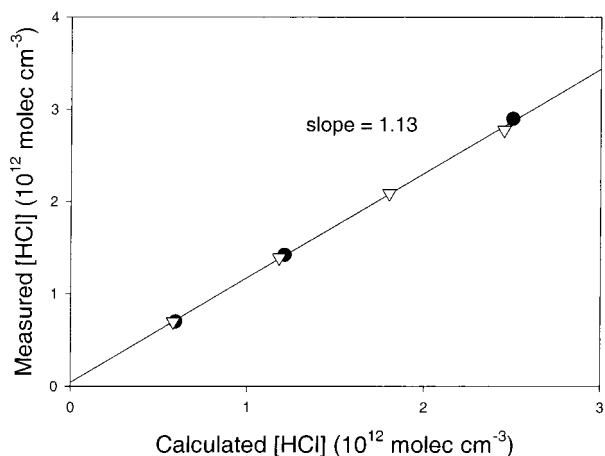


Figure 2. Comparison of measured (using infrared absorption) and calculated (from the excimer laser fluence) HCl concentration produced in the flash photolysis of a Cl₂-C₂H₆-O₂-He mixture at 40 Torr total pressure. The measurements were made both in the absence (filled symbols) or presence (open symbols) of H₂O (9.9×10^{16} molec cm⁻³). The peak HCl absorption cross sections derived from the measurements were 4.3×10^{-17} cm² molecule⁻¹ (dry) and 3.6×10^{-17} cm² molecule⁻¹ (with water).

of Cl atoms by the reaction of C₂H₅ + Cl₂ as described previously.²⁴

The amount of HCl measured using the TDL was always 12–15% higher than that calculated from the excimer laser fluence and the Cl₂ concentration. Since the excimer fluence may not be perfectly spatially homogeneous and reflections occur inside the cell, the measured HCl was used to quantify the fluence, rather than the HCl being obtained from the measured laser power. The Cl₂-C₂H₆ experiments were not performed every day, to reduce the risk of having residual C₂H₆ in the system, which could react with Cl to produce HCl. Day-to-day variations in the total excimer power exiting the cell were normalized to the previous HCl calibration. Figure 2 shows a plot of measured HCl versus calculated HCl for conditions of 40 Torr total pressure in the presence and absence of about 3 Torr water vapor. The HCl concentration measured by integrated area agrees in both cases, but is about 13% higher than calculated from the excimer fluence measured behind the cell. The precision in measuring $\sim 10^{12}$ molecules cm⁻³ of HCl was on the order of 1×10^{10} molecules cm⁻³.

Measurement of OH + ClO at 298 K. Photolysis of Cl₂-O₃-O₂-H₂O mixtures clearly led to the formation of HCl on the order of $1\text{--}4 \times 10^{10}$ molecule cm⁻³. Figure 3a illustrates the time-resolved production of HCl in an experiment at 43 Torr. The HCl measurements are 1 ms apart, as a result of ramping the diode current at a frequency of 1 kHz. After the excimer laser pulse occurs at a delay of 6.8 ms, a clear increase in the HCl concentration is observed. Figure 3b gives a composite of the spectrally resolved HCl peak, obtained by co-adding the diode laser sweeps before and after the excimer pulse and then subtracting the former from the latter to remove residual baseline oscillations. The HCl concentration was measured relative to the gently sloping baseline.

Under the conditions used, HCl can be formed both by the primary reaction, OH + ClO, and by secondary reactions. Under the experimental conditions used, secondary production was similar in magnitude to that from reaction 3b, but the sensitivity was sufficiently high to determine 3b reasonably accurately. Secondary production of HCl can occur from two sources: reaction of Cl with impurities in the system, or from reactions that are intrinsic to the source chemistry and thus cannot easily

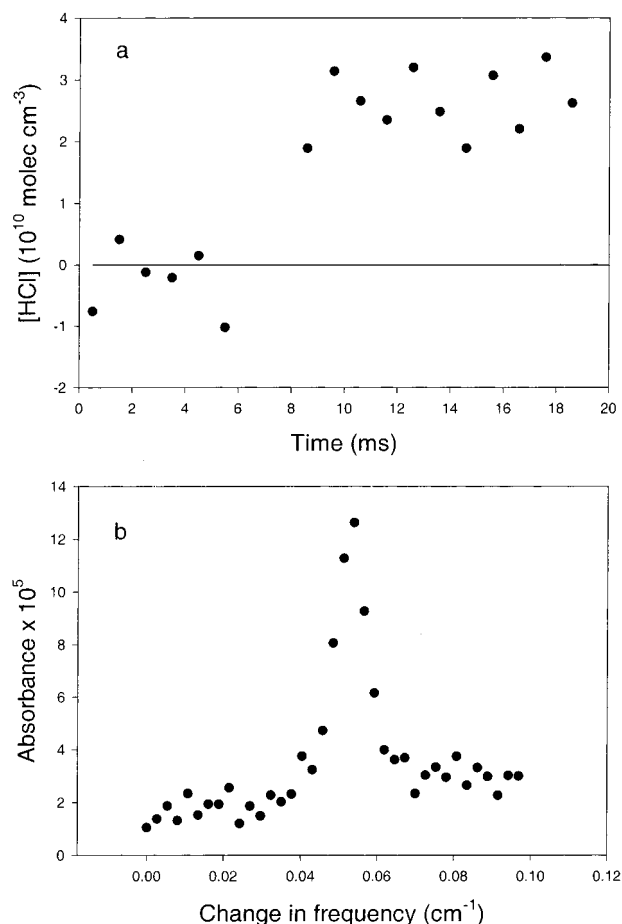
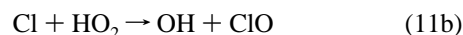
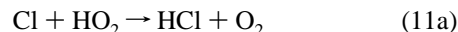


Figure 3. Measurement of HCl formed in the flash photolysis of Cl₂ (5.3×10^{15}), O₃ (6.5×10^{15}), and H₂O (9.6×10^{16}) molecule cm⁻³ at a total pressure of 42.9 Torr (5.1 Torr O₂, balance He). (a) Time series showing production of 3.0×10^{10} molecule cm⁻³ of HCl. The excimer laser fired at 6.8 ms. Average from 60 excimer pulses. (b) Composite showing spectrally resolved HCl peak, obtained by subtracting co-added sweeps before excimer pulse from co-added sweeps after excimer pulse.

be avoided. The reaction of Cl atoms with impurities was shown not to be a serious problem from experiments involving the photolysis of Cl₂-O₂-H₂O. In the presence of about 5×10^{12} Cl atoms cm⁻³, less than 5×10^{10} molecule cm⁻³ of HCl were produced. Assuming that the chlorine atoms were in excess, the latter value gives an estimate of the impurity (presumably organic) present



In the presence of 1×10^{16} molecule cm⁻³ O₃, though, the Cl atoms would react exclusively with O₃, so the HCl would be well below the detection limit for this study and would be formed with a time constant on the order of 1 μs, controlled by Cl + O₃. Control experiments were performed using different combinations of the gases Cl₂, H₂O, and O₃, but no evidence was found for extraneous HCl sources that would impact the chemistry of reaction 3. Other secondary sources of HCl, such as the reaction of Cl with HO₂, were shown by computer modeling to be much smaller than that discussed above, i.e., $< 5 \times 10^8$ molecule cm⁻³



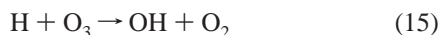
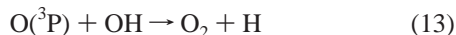
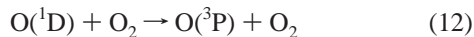
The production of HCl by intrinsic chemistry was a much more

TABLE 1: Major Reactions Describing the Production of HCl

reaction	rate coefficient at 298 K ^{a,b}
$O_3 + h\nu \rightarrow O(^1D) + O_2$	$\Phi(O) = 0.78$
$O_3 + h\nu \rightarrow O(^3P) + O_2$	$\Phi(O) = 0.22$
$Cl_2 + h\nu \rightarrow Cl + Cl$	$\Phi(Cl) = 2.0$
$O(^1D) + H_2O \rightarrow OH + OH$	2.2×10^{-10}
$O(^1D) + O_2 \rightarrow O(^3P) + O_2$	4.0×10^{-11}
$Cl + O_3 \rightarrow ClO + O_2$	1.2×10^{-11}
$OH + ClO \rightarrow HO_2 + Cl$	1.8×10^{-11}
$OH + ClO \rightarrow HCl + O_2$	1.25×10^{-12} (c)
$O(^3P) + OH \rightarrow H + O_2$	3.3×10^{-11}
$O(^3P) + Cl_2 \rightarrow ClO + Cl$	4.2×10^{-14}
$O(^3P) + ClO \rightarrow Cl + O_2$	3.8×10^{-11}
$OH + Cl_2 \rightarrow HOCl + Cl$	6.3×10^{-14} (d)
$OH + O_3 \rightarrow HO_2 + O_2$	7.8×10^{-14}
$Cl + HO_2 \rightarrow HCl + O_2$	3.2×10^{-11}
$Cl + HO_2 \rightarrow OH + ClO$	9.0×10^{-12}
$H + O_3 \rightarrow OH + O_2$	2.9×10^{-11}
$H + Cl_2 \rightarrow HCl + Cl$	1.9×10^{-11} (e)

^a Rate coefficient units are $\text{cm}^3 \text{ molecule}^{-1} \text{ s}^{-1}$. ^b Taken from ref 29 unless noted. ^c This work. ^d Weighted mean of literature values. ^e From Michael and Lee,³⁸ Bemand and Clyne,³⁹ and Wagner et al.⁴⁰

difficult problem to overcome, and the amount of HCl from these reactions was roughly equal to that produced from reaction 3b. The major source was linked to the presence of $O(^3P)$ atoms, which were produced both in the photolysis of O_3 (reaction 5b, yield 20%) and by quenching of $O(^1D)$ by O_2

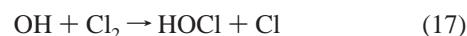


Quenching of $O(^1D)$ was minimized by keeping the ratio $[H_2O]/[O_2]$ as high as possible. Unfortunately, since the rate determining step in the production of this secondary HCl was the reaction of $O(^3P)$ with OH, production from $H + Cl_2$ and from $OH + ClO$ occurred on the same time scale, so computer modeling was required to derive the rate coefficient. The reactions listed in Table 1 summarize the major competitive loss reactions of $O(^1D)$, Cl, OH, and H. This subset of reactions essentially describes the formation of HCl for the conditions used. The complete reaction scheme used in the numerical model (Achem³⁵) contained about 50 reactions, including ground and electronically excited states of O and O_2 . Rate coefficients were taken from the JPL²⁹ or IUPAC³⁶ evaluations whenever possible, and pressure-dependent rate coefficients were estimated for the appropriate pressure of helium where exact values were not available. However, the pressure-dependent reactions ($H + O_2$ and $O + O_2$) did not play a great role at 30–40 Torr, so accurate values of the rate coefficients were not necessary.

For the reaction of OH with Cl_2 , a weighted average of the values in the literature was used, which gave a rate coefficient of $6.3 \times 10^{-14} \text{ cm}^3 \text{ molecule}^{-1} \text{ s}^{-1}$ (6% greater than the most recent measurement by Gilles et al.³⁷). For $H + Cl_2$, the direct studies of Michael and Lee, Bemand and Clyne, and Wagner et al. are in good agreement.^{38–40} A value of $1.9 \times 10^{-11} \text{ cm}^3 \text{ molecule}^{-1} \text{ s}^{-1}$ was chosen as the average of the room-temperature rate coefficients from these studies. The overall rate coefficient for reaction 3 was set to $1.9 \times 10^{-11} \text{ cm}^3 \text{ molecule}^{-1} \text{ s}^{-1}$, the currently recommended value.²⁹ However, as will be shown later, the HCl yield is not strongly dependent on this

value, since the OH decay is largely controlled by O_3 and Cl_2 . The excimer fluence used in the model was corrected for absorption down the length of the cell by Cl_2 and O_3 , the calculated fluence at the center of the cell being used in the model. Corrections were always less than 6%. For the $Cl_2-C_2H_6$ experiments, the sample was always optically thin at 308 nm, so this gave a measure of the incident fluence.

Under the conditions used, the decay rate of OH radicals was largely controlled by the reactions $OH + O_3$ and $OH + Cl_2$, and the loss rate for OH decay was between 600 and 1000 s^{-1}



In fact, only about 20–40% of the OH actually reacted with ClO for any experiment. However, this essentially means that the rate of production of HCl is being measured against the rate of reaction of OH with Cl_2 and O_3 , two reactions for which the rate coefficient is reasonably well-known. Thus, the values of k_{3b} reported here are to a large extent independent of the value of k_3 , which is still uncertain to $\pm 20\%$.

Experiments on a given day were conducted with fixed flows of O_3 and H_2O , varying the Cl_2 over a range of flows (usually a factor of 3 or 4). The experimental conditions used and results obtained are summarized in Table 2. In addition to the various concentrations, Table 2 gives the total change in measured HCl (estimated precision $\pm 20\%$), the modeled contributions from reactions 3 and 14, and the rate coefficient k_{3b} required to reproduce the measured [HCl]. The initial [OH], derived from the complete model, was around $1.8-2.1 \times 10^{12} \text{ molecule cm}^{-3}$, while the ClO was varied in the range $2.4-9.7 \times 10^{12} \text{ molecule cm}^{-3}$. The range of k_{3b} reported is fairly small, despite a wide change in initial [ClO], leading to confidence in the measurements. The unweighted mean of the 27 determinations shown in Table 2 is $(1.23 \pm 0.25) \times 10^{-12} \text{ cm}^3 \text{ molecule}^{-1} \text{ s}^{-1}$, which is a branching ratio of 6.5% expressed relative to the recommended overall rate coefficient k_3 .²⁹ Figure 4 shows the measured HCl as a function of [ClO] at 30 and 40 Torr with lines indicating the HCl level expected for 0, 5% and 10% yields. The lines are derived from computer simulations beginning with typical values of $O(^1D)$ and H_2O at each pressure. The exact HCl produced will depend on the particular combination of conditions, but the lines give an indication of the magnitude and trend to be expected with the given variation in [ClO]. As can be seen, the total HCl produced for a given O_3 and H_2O is largely independent of the [ClO]. This can be rationalized since the OH also reacts with O_3 and Cl_2 , and the ClO is proportional to the Cl_2 concentration. Thus, the partitioning of OH reactivity between Cl_2 and ClO does not change markedly as the Cl_2 concentration is increased. Likewise, the secondary HCl from $H + Cl_2$ (given by the lines marked 0% in Figures) is largely independent of [ClO] because the competition between $O + ClO$ and $O + OH$ and between $H + Cl_2$ and $H + O_3$ tend to offset one another. The fact that the observed yields of HCl are relatively independent of [ClO] (and hence $[Cl]_0$) also suggests that the HCl is not being formed in reactions of Cl atoms with impurities and that secondary chemistry has been adequately accounted for.

Reactions of Excited Species. The potential exists for several species (OH, ClO, HCl) to be produced in vibrationally excited states, which may have an effect on the chemistry or detection of these species. The primary source of OH is the reaction of $O(^1D)$ with H_2O , which produces OH radicals in vibrational levels up to $v = 3$.⁴¹ The present experiments were conducted

TABLE 2: Summary of Experimental Conditions and Results at 296 K

pressure (Torr)	O ₃ ^a (10 ¹⁵ cm ⁻³)	Cl ₂ (10 ¹⁵ cm ⁻³)	H ₂ O (10 ¹⁶ cm ⁻³)	OH ^b (10 ¹² cm ⁻³)	ClO ^c (10 ¹² cm ⁻³)	HCl _{meas} (10 ¹⁰ cm ⁻³)	HCl ^d (OH+ClO)	HCl ^e (H+Cl ₂)	k _{3b} (10 ⁻¹²)	
31	4.69	4.07	6.45	1.93	4.5	2.80	1.12	1.68	0.92	
	4.66	5.39	6.41	1.85	5.8	3.44	1.85	1.59	1.43	
	4.72	2.73	6.49	1.95	3.1	2.82	1.26	1.56	1.27	
	4.65	6.72	6.40	1.80	7.0	3.06	1.54	1.52	1.12	
	4.61	8.67	6.34	1.72	8.8	3.06	1.69	1.37	1.21	
	4.68	4.06	6.43	1.92	4.5	2.65	0.99	1.66	0.82	
	4.65	6.05	6.40	1.82	6.5	3.58	2.03	1.55	1.53	
	4.68	4.73	6.43	1.88	5.1	3.40	1.78	1.62	1.43	
	4.64	7.38	6.38	1.77	7.6	3.62	2.14	1.48	1.51	
	4.66	5.39	6.41	1.84	5.8	3.03	1.44	1.59	1.11	
	4.68	4.06	6.43	1.89	4.5	2.91	1.29	1.62	1.10	
	4.66	3.77	6.50	1.99	4.3	3.05	1.31	1.74	1.06	
	43	6.47	5.23	9.55	2.07	4.5	3.07	1.66	1.41	1.60
		6.42	7.80	9.48	1.99	6.5	2.35	0.98	1.37	0.84
6.40		10.3	9.44	1.92	8.5	2.85	1.58	1.27	1.28	
6.56		2.65	9.68	2.19	2.4	2.16	0.93	1.23	1.23	
6.48		5.25	9.57	2.08	4.5	3.00	1.58	1.42	1.52	
6.47		8.73	9.55	1.99	7.1	3.09	1.74	1.35	1.44	
6.44		11.3	9.51	1.92	9.0	2.88	1.63	1.25	1.30	
6.51		7.90	9.61	2.02	6.5	2.94	1.55	1.39	1.31	
6.59		5.33	9.73	2.11	4.5	2.84	1.41	1.43	1.33	
38		4.95	10.7	8.95	1.75	9.7	2.35	1.19	1.16	0.86
	4.75	5.15	8.60	1.86	5.0	2.31	0.97	1.34	0.83	
	4.71	8.51	8.51	1.75	7.9	3.20	1.92	1.18	1.55	
	4.89	7.07	9.51	1.91	6.7	3.24	1.93	1.31	1.48	
	4.92	3.55	9.56	2.00	3.6	2.55	1.20	1.35	1.16	
	4.86	7.90	9.45	1.88	7.4	2.55	1.28	1.27	0.95	

^a O₃ = 0.038 × O₂. ^b OH from model extrapolated back to zero time. ^c ClO from model at roughly half of OH decay. ^d Modeled HCl produced from OH + ClO (10¹⁰ cm⁻³). ^e Modeled HCl produced from H + Cl₂ (10¹⁰ cm⁻³).

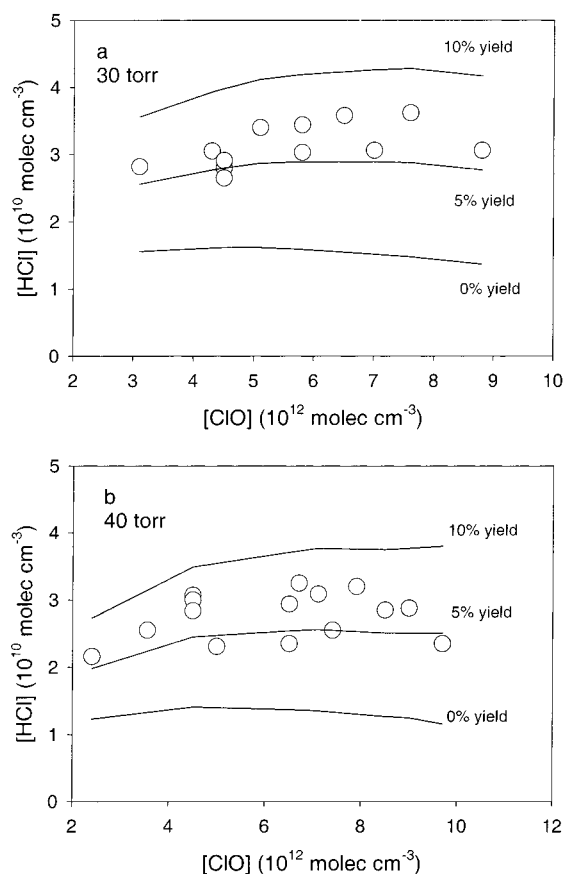


Figure 4. Measured [HCl] plotted as a function of [ClO] at (a) ~30 and (b) ~40 Torr total pressure. The lines indicate the level of HCl expected to be formed for 0% (secondary production only), 5%, and 10% yields of HCl in reaction 3b. The initial [OH] was around 2 × 10¹² molecule cm⁻³.

in the presence of 2 Torr of water vapor. Quenching of OH(*v*) by H₂O is known to be fast (>1 × 10⁻¹¹ cm³ molecule⁻¹

s⁻¹),⁴¹⁻⁴³ and the OH is expected to be fully relaxed within 2 μs. Some secondary production of OH by H + O₃ occurs, leading to OH excited up to *v* = 9. However, higher vibrational levels of OH should be quenched very rapidly by both O₂ and H₂O,^{41,43,44} and the computer model shows that the amount of H produced is in any case very small compared to the primary OH source.

The reaction of Cl atoms with O₃ produces vibrationally excited ClO.⁴⁵ Quenching of ClO(*v*) has not been studied widely. Rate coefficients for vibrational quenching of ClO by Cl₂ and O₃ are thought to be around 2 × 10⁻¹² cm³ molecule⁻¹ s⁻¹, and complete vibrational quenching of ClO to the *v* = 0 state should be complete for our conditions within 200 μs, based on the data in Figure 5 of Matsumi et al.⁴⁵ Several groups have commented on the possibility of the reaction of Cl with vibrationally excited ClO, which can lead to incomplete conversion of Cl atoms to ClO when reaction 6 is used.^{23,46} Such studies tended to be in low pressure flow tubes. The effect will probably not be important here as a result of the high overall pressures and high [O₃] used, which leads to a chemical lifetime for Cl of a few microseconds. Thus, conversion of Cl into ClO should be quantitative. It is not known what effect vibrationally excited ClO would have on the OH + ClO reaction, although vibrational energy would be expected to inhibit the reaction, since the overall *k* has a negative activation energy.²⁹

Finally, the product HCl could be formed in excited vibrational states (*v* < 4 if singlet O₂ is formed). The extended geometry of the transition state also suggests vibrational excitation of the HCl product.^{47,48} Quenching of HCl(*v*) by H₂O is rapid, though, *k* = 1.5 × 10⁻¹¹ cm³ molecule⁻¹ s⁻¹,⁴⁹ and no excited HCl should remain on the time scale of the diode laser measurements.

Sensitivity Tests. The most critical experimental parameter in the determination is probably the measurement of the excimer laser fluence, since it essentially enters into the rate coefficient *k*_{3b} quadratically (since it is linked to both the OH and ClO concentrations). Thus, even though the fluence is calibrated in

situ relative to HCl production, relative errors do not cancel (as they would in a straightforward quantum yield experiment) since the calibration reaction is first order and the reaction under study is second order. However, the fact that the HCl line strength is very well-known constrains the fluence more tightly than a direct measurement of laser power would.

The rate coefficient k_{3b} derived here is in essence measured relative to $\text{OH} + \text{Cl}_2$ and $\text{OH} + \text{O}_3$ and is not particularly sensitive to the overall value of k_3 . To test this, computer simulations were run with k_3 10% higher or lower; the calculated HCl concentration changed by less than 1%. Further tests were conducted with the rate coefficients for $\text{H} + \text{Cl}_2$, $\text{OH} + \text{O}_3$, and $\text{OH} + \text{Cl}_2$ adjusted separately and together. As expected, an increase in $\text{H} + \text{Cl}_2$ led to an increase in the amount of secondary HCl produced, requiring a lower value of k_{3b} to match the experimental data. The effect was most pronounced at low $[\text{Cl}_2]$ where H atoms react mostly with O_3 . The simulations indicated that if the rate coefficient is as high as $2.2 \times 10^{-11} \text{ cm}^3 \text{ molecule}^{-1} \text{ s}^{-1}$, k_{3b} could be reduced to $1.15 \times 10^{-12} \text{ cm}^3 \text{ molecule}^{-1} \text{ s}^{-1}$. Increases in both $\text{OH} + \text{O}_3$ and $\text{OH} + \text{Cl}_2$ resulted in an increased loss rate for OH, and consequently less occurrence of $\text{O} + \text{OH}$. The decreased amount of secondary OH required an increase in k_{3b} . The recommended rate coefficient for $\text{OH} + \text{O}_3$ has recently been revised upward from 6.8×10^{-14} to $7.8 \times 10^{-14} \text{ cm}^3 \text{ molecule}^{-1} \text{ s}^{-1}$.²⁹ A 10% change in either $\text{OH} + \text{O}_3$ or $\text{OH} + \text{Cl}_2$ led to 4–5% changes in k_{3b} in the same direction. The combined uncertainty in the HCl yield related to the kinetics parameters is thus estimated as being around 20%, similar to the random error in the determinations and the uncertainty due to the excimer fluence. Thus, we estimate an overall uncertainty of 35%, leading to a value of $k_{3b} = (1.25 \pm 0.45) \times 10^{-12} \text{ cm}^3 \text{ molecule}^{-1} \text{ s}^{-1}$. Expressed as a branching ratio, this becomes $(6.5 \pm 3.0)\%$ relative to the recommended²⁹ overall rate coefficient of $1.9 \times 10^{-11} \text{ cm}^3 \text{ molecule}^{-1} \text{ s}^{-1}$, where an uncertainty of $\pm 25\%$ in the overall rate coefficient has been included.

Other Experimental Tests. A number of other experiments were conducted to confirm that the HCl was being produced from the reactions 3 and 14. Some experiments were attempted using a faster diode laser sweep rate (4 kHz) to improve the time resolution. Production of HCl occurred on a time scale consistent with that predicted by the model, but the data were not of sufficient quality to obtain any kinetic information. However, the HCl was clearly produced on a time scale of 100s of μs , too long for it to be due to reaction of Cl atoms with impurities, since Cl atoms are scavenged extremely rapidly by O_3 .

Experiments were also conducted at 265 and 333 K (unfortunately hampered by cracks in the cell window). The amount of HCl produced at lower temperature, for otherwise identical conditions, was more than at room temperature. This can be rationalized in terms of the temperature dependences of the major reactions. Reactions 16 and 17, which consume OH, both have normal temperature dependences,^{29,36} while reaction 3 has a negative temperature dependence, so the fraction of OH reacting with ClO should be higher at 265 K. Again, the dependence of the HCl on experimental conditions points toward its being formed from reaction 3, but uncertainties in the cell pressure caused by the leak preclude further analysis.

Discussion

The results presented here clearly show that HCl is formed in reaction 3 with a yield of 6–7% (based on the currently recommended rate coefficient). The observation of small, but

significant amounts of HCl is in accord with three other recent studies.^{20,22,23} The methodology in the current study differs from the previous ones in that a slowly flowing mixture is used with a pulsed radical production. While wall reactions were minimized in the present study, the presence of large radical concentrations led to an increased contribution from secondary chemistry. However, the results agree very well with those obtained using discharge-flow techniques.

Four other groups have attempted to measure the HCl yield directly. Poulet et al.¹⁷ used a traditional discharge-flow system, with electron-impact mass spectrometric detection. They measured HCl in pairs of experiments with either Cl atoms or O_3 in excess. All of the HCl observed could be accounted for by reactions such as $\text{Cl} + \text{HO}_2$, and a branching fraction of $(2 \pm 12)\%$ was quoted. The determination suffered from variable backgrounds of HCl from the Cl_2 discharge, and uncertainties in the amount of OH and Cl probably also played a role.

Lipson et al.^{18,22} made two determinations of the HCl production rate, the former using deuterated hydroxyl radicals, OD (to discriminate against background levels of HCl) and the latter using OH. The studies were conducted in a high-pressure turbulent flow tube at pressures between 100 and 200 Torr, which should minimize wall contact. A background of HCl was present and the change in HCl was measured above this level. The reaction was not driven to completion, and the rate of HCl production was equated to the rate of OH loss. Absolute calibrations were required for ClO, OH, and HCl using chemical ionization mass spectrometry. It should be noted that the overall rate coefficient measured by Lipson et al. is 30% lower than the currently recommended value and up to 40% lower than the most recent determinations.^{19–21} It is not clear whether there is a systematic calibration error that propagates into both the overall rate coefficient and the branching fraction. Lipson et al. quote a rate coefficient k_{3b} of $(9.5 \pm 1.6) \times 10^{-13} \text{ cm}^3 \text{ molecule}^{-1} \text{ s}^{-1}$ at room temperature, which is similar to that measured here. Expressed relative to their overall rate coefficient, this corresponds to a branching fraction of 7%, or 5% relative to the NASA-JPL recommended value of k_3 ;²⁹ this determination is also the basis for the current recommendation for k_{3b} .

Wang and Keyser²³ used a low-pressure discharge flow tube and measured HCl using a tunable diode laser. They also measured the initial OH concentration and the ClO, using resonance fluorescence and UV absorption, respectively. The method did not require a knowledge of the overall rate coefficient, since it involved the complete reaction of OH with ClO, and a determination of the ratio of HCl produced to the initial OH. However, secondary production of HCl occurred, and the quoted branching fraction $(9.0 \pm 4.8)\%$ was obtained by extrapolating the HCl back to zero OH. Expressed relative to the overall reaction, a rate coefficient $k_{3b} = 1.7 \times 10^{-12} \text{ cm}^3 \text{ molecule}^{-1} \text{ s}^{-1}$ is obtained, which is somewhat larger than both the present measurement and that of Lipson et al.²² The very recent study of Bedjanian et al., which used a low-pressure discharge flow tube, gave the lowest yield of HCl from the recent studies, 3.5% at 298 K.²⁰

Overall, the four most recent determinations clearly show the occurrence of channel 3b. The studies of Lipson et al.,²² Wang and Keyser,²³ and Bedjanian et al.,²⁰ which covered wider temperature ranges than the present study, indicate that the HCl yield is largely independent of both temperature and pressure down to 220 K. There is also good evidence from theoretical calculations of a low energy pathway to give $\text{HCl} + \text{O}_2$ on a singlet surface,^{22,47} although a third theoretical study found the

transition state to be too energetic to allow any reaction.⁴⁸ The agreement between the measurements of k_{3b} is only about a factor of 2 if each determination is taken as reported, although the actual agreement is probably better. Each determination has potential problems with calibration and background levels of HCl, which were all addressed differently. The present technique uses a different approach from the others, incorporating rapid time response on a time scale shorter than that for diffusion to the walls. The determination used an absolute calibration of HCl based on known spectroscopic constants and also tied the determination of excimer laser fluence to the HCl measurement. However, the complexity of the chemistry, coupled with the need to numerically simulate the results, leads to an additional uncertainty. A further weakness of this study is that neither OH or ClO was measured, but the calculation of their concentration is tied very closely to the HCl calibration. An ideal measurement might utilize a flowing discharge source of ClO with in situ UV detection,¹⁹ and flash production of OH coupled with time-resolved diode laser detection of HCl as used here.

In the atmosphere, the concentrations of OH and ClO are controlled by reactions other than reaction 3. Thus, for atmospheric models the absolute rate coefficient for reaction 3b is required, rather than a branching ratio. The recent determinations of k_{3b} confirm that HCl production occurs at a level of significance to stratospheric chemistry.^{9–12} However, there is still a factor of 2 discrepancy in the rate coefficients for reaction 3b as reported by the individual groups. This may represent real systematic differences between the studies, or may simply reflect the difficulties inherent in measuring this parameter.

Acknowledgment. This work was supported by NASA's Upper Atmosphere Research Program. C. S. Kegley-Owen held a NSF Training Grant (EAR-9256339) during preliminary stages of the work. The authors thank Michael Coffey and Dirk Richter of NCAR for comments on the manuscript. NCAR is sponsored by the National Science Foundation.

References and Notes

- (1) *Scientific Assessment of Ozone Depletion: 1998*; World Meteorological Organization: Geneva, 1999.
- (2) Brasseur, G. P.; Orlando, J. J.; Tyndall, G. S., Eds. In *Atmospheric Chemistry and Global Change*; Oxford University Press: New York, 1999.
- (3) Finlayson-Pitts, B. J.; Pitts, J. N., Jr. *Chemistry of the Upper and Lower Atmosphere*; Academic Press: San Diego, 2000.
- (4) Brasseur, G.; De Rudder, A.; Tricot, C. *J. Atmos. Chem.* **1985**, *3*, 261.
- (5) McElroy, M. B.; Salawitch, R. J. *Science* **1989**, *243*, 763.
- (6) Toumi, R.; Bekki, S. *Geophys. Res. Lett.* **1993**, *20*, 2447.
- (7) Chandra, S.; Jackman, C. H.; Douglass, A. R.; Fleming, E. L.; Considine, D. B. *Geophys. Res. Lett.* **1993**, *20*, 351.
- (8) Natarajan, M.; Callis, L. B. *J. Geophys. Res.* **1991**, *96*, 9361.
- (9) Michelsen, H. A., et al. *Geophys. Res. Lett.* **1996**, *23*, 2361.
- (10) Chance, K.; Traub, W. A.; Johnson, D. G.; Jucks, K. W.; Ciarpallini, P.; Stachnik, R. A.; Salawitch, R. J.; Michelsen, H. A. *J. Geophys. Res.* **1996**, *101*, 9031.
- (11) Khosravi, R.; Brasseur, G. P.; Smith, A. K.; Rusch, D. W.; Waters, J. W.; Russell, J. M., III. *J. Geophys. Res.* **1998**, *103*, 16203.
- (12) Lary, D. J.; Chipperfield, M. P.; Toumi, R. *J. Atmos. Chem.* **1995**, *21*, 61.
- (13) Leu, M. T.; Lin, C. L. *Geophys. Res. Lett.* **1979**, *6*, 425.
- (14) Ravishankara, A. R.; Eisele, F. L.; Wine, P. H. *J. Chem. Phys.* **1983**, *78*, 1140.
- (15) Hills, A. J.; Howard, C. J. *J. Chem. Phys.* **1984**, *81*, 4458.
- (16) Burrows, J. P.; Wallington, T. J.; Wayne, R. P. *J. Chem. Soc., Faraday Trans. 2* **1984**, *80*, 957.
- (17) Poulet, G.; Laverdet, G.; Le Bras, G. *J. Phys. Chem.* **1986**, *90*, 159.
- (18) Lipson, J. B.; Elrod, M. J.; Beiderhase, T. W.; Molina, L. T.; Molina, M. J. *J. Chem. Soc., Faraday Trans.* **1997**, *93*, 2665.
- (19) Kegley-Owen, C. S.; Gilles, M. K.; Burkholder, J. B.; Ravishankara, A. R. *J. Phys. Chem. A* **1999**, *103*, 5040.
- (20) Bedjanian, Y.; Riffault, V.; Le Bras, G. *Int. J. Chem. Kinet.* **2001**, *33*, 587.
- (21) Wang, J. J.; Keyser, L. F. *J. Phys. Chem. A* **2001**, *105*, 10544.
- (22) Lipson, J. B.; Beiderhase, T. W.; Molina, L. T.; Molina, M. J.; Olzmann, M. *J. Phys. Chem. A* **1999**, *103*, 6540.
- (23) Wang, J. J.; Keyser, L. F. *J. Phys. Chem. A* **2001**, *105*, 6479.
- (24) Kegley-Owen, C. S.; Tyndall, G. S.; Orlando, J. J.; Fried, A. *Int. J. Chem. Kinet.* **1999**, *31*, 766.
- (25) Stickel, R. E.; Nicovich, J. M.; Wang, S.; Zhao, Z.; Wine, P. H. *J. Phys. Chem.* **1992**, *96*, 9875.
- (26) Rim, K. T.; Hershberger, J. F. *J. Phys. Chem. A* **1999**, *103*, 3721.
- (27) Cantrell, C. A.; Zimmer, A.; Tyndall, G. S. *Geophys. Res. Lett.* **1997**, *24*, 2195.
- (28) *CRC Handbook of Chemistry and Physics*, 65th ed.; Weast, R. C., Ed.; CRC Press: Boca Raton, FL, 1985.
- (29) Sander, S. P.; Friedl, R. R.; DeMore, W. B.; Golden, D. M.; Kurylo, M. J.; Hampson, R. F.; Huie, R. E.; Moortgat, G. K.; Ravishankara, A. R.; Kolb, C. E.; Molina, M. J. JPL Publication 00-003; NASA Jet Propulsion Laboratory: Pasadena, CA, 2000.
- (30) Rothman, L. S.; et al. *J. Quant. Spectrosc. Radiat. Transfer* **1998**, *60*, 665.
- (31) Pine, A. S.; Fried, A.; Elkins, J. W. *J. Mol. Spectrosc.* **1985**, *109*, 30.
- (32) Pine, A. S.; Looney, J. P. *J. Mol. Spectrosc.* **1987**, *122*, 41.
- (33) Babrov, H.; Ameer, G.; Benesch, W. *J. Chem. Phys.* **1960**, *33*, 145.
- (34) Rank, D. H.; Eastman, D. P.; Rao, B. S.; Wiggins, T. A. *J. Mol. Spectrosc.* **1963**, *10*, 34.
- (35) Braun, W.; Herron, J. T.; Kahaner, D. K. *Int. J. Chem. Kinet.* **1988**, *20*, 51.
- (36) Atkinson, R.; Baulch, D. L.; Cox, R. A.; Hampson, R. F., Jr; Kerr, J. A.; Rossi, M. J.; Troe, J. *J. Phys. Chem. Ref. Data* **1997**, *26*, 521.
- (37) Gilles, M. K.; Burkholder, J. B.; Ravishankara, A. R. *Int. J. Chem. Kinet.* **1999**, *31*, 417.
- (38) Michael, J. V.; Lee, J. H. *Chem. Phys. Lett.* **1977**, *51*, 303.
- (39) Bemand, P. P.; Clyne, M. A. A. *J. Chem. Soc., Faraday Trans. 2* **1977**, *73*, 394.
- (40) Wagner, H. G.; Welzbacher, U.; Zellner, R. *Ber. Bunsen-Ges. Phys. Chem.* **1976**, *80*, 902.
- (41) Silvente, E.; Richter, R. C.; Hynes, A. J. *J. Chem. Soc., Faraday Trans. 1997*, *93*, 2821.
- (42) Smith, I. W. M.; Williams, M. D. *J. Chem. Soc., Faraday Trans. 2* **1985**, *81*, 1849.
- (43) Raiche, G. A.; Jeffries, J. B.; Rensberger, K. J.; Crosley, D. R. *J. Chem. Phys.* **1990**, *92*, 7258.
- (44) Chalamala, B. R.; Copeland, R. A. *J. Chem. Phys.* **1993**, *99*, 5807.
- (45) Matsumi, Y.; Nomura, S.; Kawasaki, M.; Imamura, T. *J. Phys. Chem. A* **1996**, *100*, 176.
- (46) Burkholder, J. B.; Hammer, P. D.; Howard, C. J.; Goldman, A. J. *Geophys. Res.* **1989**, *94*, 2225.
- (47) Dubey, M. K.; McGrath, M. P.; Smith, G. P.; Rowland, F. S. *J. Phys. Chem. A* **1998**, *102*, 3127.
- (48) Sumathi, R.; Peyerimhoff, S. D. *Phys. Chem. Chem. Phys.* **1999**, *1*, 5429.
- (49) Chen, H.-L.; Moore, C. B. *J. Chem. Phys.* **1971**, *54*, 4072.